CHEN, C., ZHANG, L. and JAHANSHAHI, S. Review and thermodynamic modelling of CoO in iron silicate-based slags and calcium ferrite-based slags. *VII International Conference on Molten Slags Fluxes and Salts,* The South African Institute of Mining and Metallurgy, 2004.

Review and thermodynamic modelling of CoO in iron silicate-based slags and calcium ferrite-based slags

C.CHEN , L. ZHANG and S. JAHANSHAHI
CSIRO Minerals, Clayton South, Victoria, Australia

Published experimental data on thermodynamic behaviour of cobalt-containing slags have been reviewed and used in validating a recently developed thermodynamic model. The results from the exercise show that the model provides a reasonably good description of behaviour of cobalt in multi-component slag systems. The models for cobalt containing slags, matte and oxide solid solution phases were incorporated into CSIRO's multi-phase equilibrium (MPE) package, which was used to calculate the equilibrium distribution of cobalt between matte and slag phases under various conditions. The results agreed well with the experimental data. Furthermore, the good agreement between the calculation and the plant data indicates that the operating conditions of industrial smelting and converting processes are close to equilibrium. Two diagrams showing the effects of slag chemistry and SO_2 and O_2 partial pressures on the distribution of cobalt between phases were generated for conditions similar to smelting and converting processes. These diagrams provide some useful guidelines for developing new strategies to improve cobalt recovery.

Introduction

Cobalt is an important by-product for nonferrous smelters, and deports mostly to the converter slag. Maximizing the cobalt recovery from the slag is therefore of great interest to nonferrous smelters. Cobalt recovery depends mainly on the distribution of cobalt between matte and discard slag, although it is possible to lose a significant portion in oxide solid solution phases such as magnetite based spinel. The development of strategies for maximizing the cobalt recovery can, therefore, be assisted through using models for predicting the cobalt distribution between phases.

Over the past decade, a modelling package for the calculation of multi-phase equilibrium (MPE) in metallurgical systems has been developed at CSIRO Minerals[1,2]. For the purpose of extending the capability of the MPE package to the cobalt-containing system, systematic evaluations of the available phase diagrams and thermodynamic data for six CoO-containing binary systems have been conducted. An optimized self-consistent thermodynamic database for predicting the cobalt behaviour in slag and solid solutions has been developed[3]. The developed database was also validated against published ternary phase diagram information for the CoO-Fe_3O_4-SiO_2 and the CoO-Al_2O_3-SiO_2 systems[3].

In the present study, the database has been validated against the published thermodynamic information on high order systems containing cobalt. The information includes the activity coefficient of CoO in multi-component industrial type slag systems, as well as the distribution of cobalt between slag and matte phases. Furthermore, the application of the current database to predict the cobalt distribution between matte and slag phases under various operating conditions has been examined and presented here.

CoO Activity in multi-component slag system

The activity coefficient of cobalt in slags has been measured through numerous studies using the alloy-slag-gas equilibrium experiments. These efforts have been concentrated on two type of slags commonly encountered in metallurgical processes, i.e. the iron silicate-based slags and the calcium ferrite-based slags[4-18]. The available experimental data on activity of CoO in slag systems are summarized in Table I.

Iron silicate-based slag

For the iron silicate-based slags, some experiments[4-7] were performed in silica crucibles corresponding to the condition of silica-saturation. Other studies[8-10] were performed in cobalt or platinum crucibles, or by using the levitation melting technique, which permits the iron to silica ratio to be changed in the slag. Grimsey and Toguri[6] evaluated the data of Wang *et al.*[4,5]. They gave the following expression, which related the activity coefficient of CoO, referred to as solid CoO in the silica-saturated slags to the cobalt content of Co-Cu alloys at temperatures of 1250ºC, 1300ºC and 1350ºC and cobalt concentration in slag less than 10 wt pct.

$$\gamma_{CoO} = 1.94 + 0.123[wt\ \ pct\ \ Co]_{alloy} \qquad [1]$$

Thus, when the cobalt concentration in the alloy approaches zero, the value of the activity coefficient of CoO in the slag becomes 1.94. Grimsey and Liu[7] studied the solubility of CoO in silica-saturated iron silicate slag and reported a value of the activity coefficient of CoO, referred to solid CoO, of 0.91. In the present study, the experimental data by Wang *et al.*[4,5] was not used to validate the database as the insufficient experimental details

Table I
Available activity of CoO in various slag systems

Experimental system		Temperature	Additive	CoO		
Slag	**Alloy**	**(ºC)**	**(wt%)**	**(wt%)**	**P_{O_2}/atm**	**Ref.**
CoO-Fe_xO-SiO_2 Sat.	Co-Au-Fe	1300		<10	10^{-9}~10^{-10}	7
CoO-Fe_xO-SiO_2	Co-Fe	1300		8~13	10^{-9}~10^{-10}	8
CoO-Fe_xO-SiO_2	Co-Pt-Fe	1300		3~10	10^{-7}~10^{-8}	9
CoO-Fe_xO-SiO_2	Co-Cu-Fe	1255~1378		<23	10^{-7}~10^{-10}	10
CoO-Fe_xO-SiO_2-CaO	Co-Au-Fe	1300	CaO, 3~13	5~8	10^{-9}~10^{-10}	8
CoO-Fe_xO-SiO_2-CaO	Co-Cu-Fe	1260~1370	CaO, <40	<20	10^{-7}~10^{-9}	10
CoO-Fe_xO-SiO_2-Al_2O_3	Co-Au-Fe	1300	Al_2O_3, 4~16	1~7	10^{-9}~10^{-10}	8
CoO-Fe_xO-SiO_2-Al_2O_3	Co-Cu	1400	Al_2O_3, 15~23	<3	10^{-8}~10^{-10}	16
CoO-Fe_xO-SiO_2-MgO	Co-Au-Fe	1300	MgO, 4~10	4	10^{-9}	8
CoO-Fe_xO-CaO	Co-Pt-Fe	1300		<10	10^{-7}	18
CoO-Fe_xO-CaO	Co-Cu-Fe	1255~1350		<24	10^{-7}~10^{-9}	10
CoO-Fe_xO-CaO-SiO_2	Co-Pt-Fe	1300	SiO2, 0~20	3	10^{-7}	18

provided made the direct comparison of calculations to the experimental data impossible. The activity coefficient of CoO(s) reported by Liu and Grimsey[8] and by Teague *et al.*[9] in the silica-unsaturated slags are in good agreement and can be expressed by the following relationship:

$$\gamma_{CoO} = 1.7 - 0.021\left[wt\ \ pct\ \ SiO_2\right]_{slag} \qquad [2]$$

Extrapolating Equation [2] to the silica concentration at saturation gives a value of 0.9 for the activity coefficient of CoO, which agrees with the work by Grimsey and Liu[7]. Katyal and Jeffes[10] reported the activity coefficients of CoO in iron silicate and calcium ferrite slags at temperatures between 1250 and 1350ºC by equilibrating the slags with Co-Cu alloys using a levitation technique. The value of γ_{CoO} of iron silicate slag was reported to be unity relative to the pure liquid CoO as standard state. On converting this to pure solid cobalt oxide as standard state (as will be the case throughout this work), the activity coefficient value was recalculated to be 2. This high value of the activity coefficient of CoO could be overestimated due to limitations of the experimental technique used.

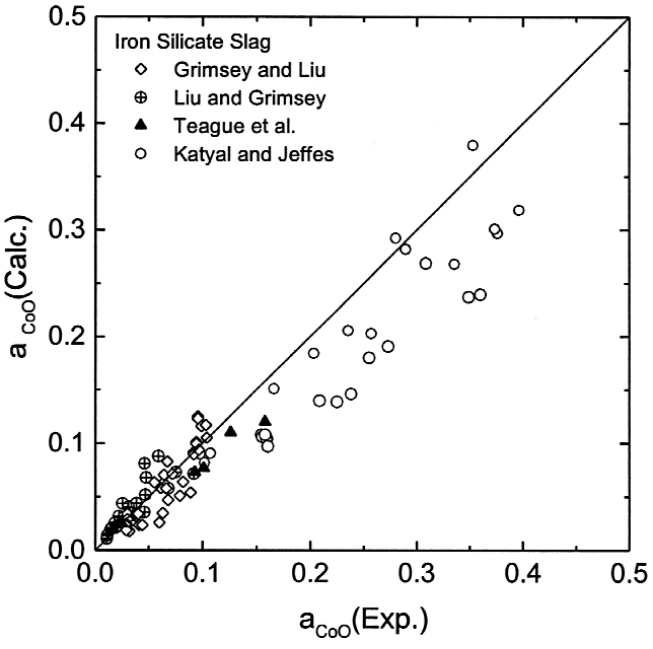

Figure 1. Comparison of measured[7-10] and calculated CoO activity in iron silica slag system

Katyal and Jeffes used a levitation melting technique in their experiment, in which the slag was heated by the heat transferred from the metal drop. As the emissivity of the slag layer is larger than that of metal drop, it is reasonable to expect that there should be a temperature gradient across the slag. Katyal and Jeffes equilibrated 1 g metal with about 85 mg of slag sample in their experiments; in such a case the slag temperature could be 50~70ºC lower than the reported metal temperature. Under such conditions, the solubility of cobalt in the slag could be underestimated in their study. Therefore, the reported activity coefficient could be overestimated.

The effects of additions of lime, alumina and magnesia on the activity coefficient of CoO in iron silicate slag were investigated in several studies[8-16]. It was found that the addition of these oxides to slag decrease the solubility of cobalt in slag, thus increasing the activity coefficient of CoO in slag. However, because of the experimental details were not given in some studies[11-15], those data could not be used to validate our database. Instead, the experimental data included in Table I were used in the present study to validate model calculations.

The CoO activities in the iron silicate-based slag, including the systems with small additions of MgO, Al_2O_3 and CaO, were calculated using CSIRO's MPE model. The results are compared with the experimental data in Figures 1 and 2. As shown in these figures, the agreement between the model calculations and the measured data are reasonably good, especially in low concentrations of CoO, where the industrial relevance is greater. It is noted that some data of Katyal and Jeffes[10] were underestimated by the model calculation. The uncertainties in the temperature measurements during their experiments make it difficult to assess their experimental data. The results of the calculations also showed that the model can reproduce the experimental findings[6-14] that addition of MgO, CaO and Al_2O_3 in the slag reduce the solubility of cobalt in the slag, and hence increase the activity coefficient of CoO in the slag.

Calcium ferrite-based slag

Experimental studies on the activity coefficient of CoO in calcium ferrite slags have been reported by Takeda *et al.*[17], Katyal and Jeffes[10] and by Teague *et al.*[18]. As part of a study into the distribution of minor elements between slag

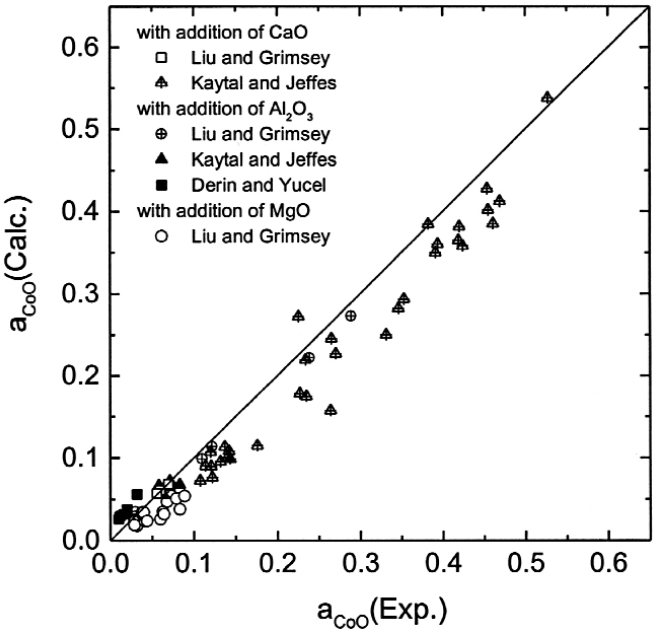

Figure 2. Comparison of measured[8,10,16] and calculated CoO activity in iron silica slag with addition of CaO, MgO and Al_2O_3

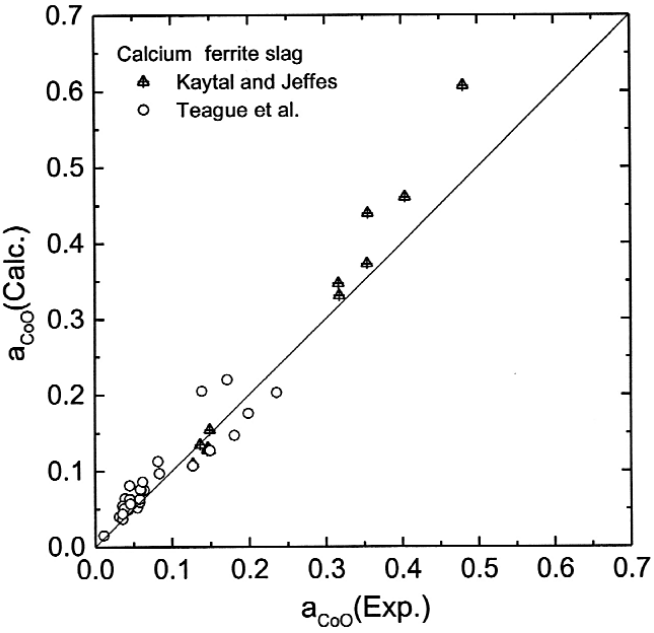

Figure 3. Comparison of measured[10,18] and calculated CoO activity in calcium ferrite slag system

and blister copper, Takeda *et al.*[17] reported the value of the activity coefficient of CoO to be about 1.4 in calcium ferrite slags at 1250ºC. Katyal and Jeffes[10] found the activity coefficient of CoO, referred to liquid CoO, was a little greater than unity in the calcium ferrite slag. Referred to solid CoO, the value of γ_{CoO} was recalculated to be 2.5. Teague *et al.*[18] reported the value of the activity coefficient of CoO to be 2.1 in the calcium ferrite slag.

The calculated CoO activity in this slag system is shown in Figure 3, together with the experimental data of Katyal and Jeffes[10] and Teague *et al.*[9,18]. A generally good agreement between them was obtained. With partial substitution of CaO by SiO_2 in the calcium ferrite slags, Teague *et al.* reported that CoO activity increases with the increasing SiO_2 content in slag up to 4 wt pct. Above this level, further increase in the SiO_2 content of the slag caused the CoO activity to decrease and spinel crystals to precipitate from the liquid slag[9,18]. As shown in Figure 4, these experimental observations were also reproduced by the model calculations. The increase of CoO activity with the increasing SiO_2 content in the calcium ferrite slag is likely to be a consequence of the very strong interactions between the CaO and the added SiO_2, which in return reduce the interactions between CoO and CaO. The precipitation of spinel crystal from the slag could decrease the CoO concentration in slag and result in the decrease of CoO activity in slag. Another possible reason for decreasing the CoO activity with increasing SiO_2 content above 4 wt pct is likely to be due to the interactions between SiO_2 and CoO.

Cobalt distribution between matte and slag

Through incorporating the Co model parameters into the MPE package, the capability of the package was extended to cobalt-containing systems and enabled prediction of the cobalt distribution between matte and slag for conditions of interest to laboratory studies and plant practice. The database for matte, which is based on a quasi-chemical model, developed by Kongoli *et al.*[19,20] was adopted in MPE.

There have been a number of investigations into the distribution of cobalt between matte and slag phases[21-30]. Analysis of the available experimental data revealed that, despite some scatter in data, they all show similar trends when plotted as the distribution coefficient of cobalt vs. matte grade. The distribution coefficient of cobalt decreases as matte grade increases. The matte-slag distribution coefficient for cobalt was defined as follows:

$$L_{Co}^{M/S} = \frac{wt\%\ Co\ in\ matte}{wt\%\ Co\ in\ slag} \qquad [3]$$

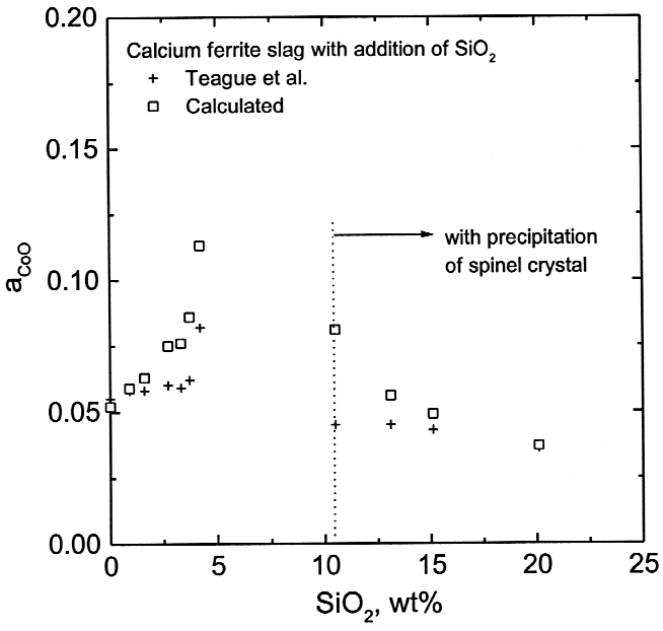

Figure 4. Comparison of measured[18] and calculated CoO activity in calcium ferrite slag system with addition of SiO_2 at 1300ºC

Table II
Comparison of experimental and calculated distribution of cobalt in industrial nickel smelting processes

Processes	wt% Co in matte		wt% Co in slag		$L_{Co}^{M/S}$		Ref.
	Exp.	Calc.	Exp.	Calc.	Exp.	Calc.	
INCO flash smelting, model 1	0.513	0.590	0.098	0.092	5.23	6.43	26
INCO flash smelting, model 2	0.572	0.682	0.110	0.116	5.20	5.88	26
INCO flash smelting, model 3	0.582	0.736	0.127	0.139	4.58	5.29	26
INCO flash smelting, model 4	0.736	0.876	0.149	0.154	4.94	5.68	26
Outokumpu flash smelting	0.760	0.810	0.140	0.146	5.42	5.54	27

Laboratory studies on cobalt distribution between matte and silica-saturated iron silicate slags, as well as the effect of the addition of CaO, MgO and Al_2O_3 in the slag, were reported by Celmer and Toguri[21] and by Choi and Cho[22]. It was found in both studies that increasing matte grade caused an increase in the cobalt content of the slag phase. The additions of the CaO, MgO and Al_2O_3 to the slag reduced the solubility of cobalt in the slag, thus increasing cobalt distribution coefficients. The reason is likely to be that the additions of these oxides to the slag reduced the interactions between the CoO and SiO_2, thus increasing the activity of CoO and decreasing the solubility of cobalt in the slag. The experimental data are compared with the calculated curves in Figures 5 and 6. The agreement is believed to be within experimental error limits.

Font *et al.*[23-25] systematically investigated the phase equilibra between both iron silicate-based slag (silica saturation, 6 wt pct of MgO) and calcium ferrite-based slag (23 wt pct CaO, 75 wt pct FeOx and 2 wt pct MgO) and Cu_2S-Ni_3S_2-FeS matte phases with varying Cu_2S or Ni_3S_2 content in the matte under controlled partial pressures of SO_2 in the gas phase. The cobalt distribution ratio between matte and slag showed a clear tendency to decrease with increasing matte grade and the ratio for calcium ferrite-based slag is lower than that for iron silicate-based slag[23,24] as shown in Figure 7. Under various Ni to Cu ratios in the matte, the relations of cobalt distribution coefficient vs. iron content in the matte were plotted in Figure 8[25]. At a specified matte grade, no obvious dependency of Co distribution coefficients on the $N_{Ni}/(N_{Ni}+N_{Cu})$ of the matte was found[25]. The measurements by Font *et al.*[23,24] also showed that at a specified matte grade, the distribution ratio of cobalt between matte and slag decreased with increasing SO_2 partial pressure, which was also reflected by the calculation. However, the calculated cobalt distribution coefficient was less sensitive to the SO_2 partial pressure than the experimental measurements. That could be caused by the insensitivity of the CoS solubility to the SO_2 partial pressure in the slag or matte models. Nevertheless, as demonstrated in Figures 7 and 8, the models are able to reproduce variations of $L_{Co}^{M/S}$ with chemistry of mattes and slags.

The measured cobalt distribution between the matte and slag phases in industrial process have been reported by a number of researchers[26-30]. For the industrial processes, where the operating parameters were provided[26,27], the comparison between the calculated cobalt distribution coefficient and the data from commercial plants are summarized in Table II and Figure 9. This Figure shows the relation between the cobalt distribution coefficient and the

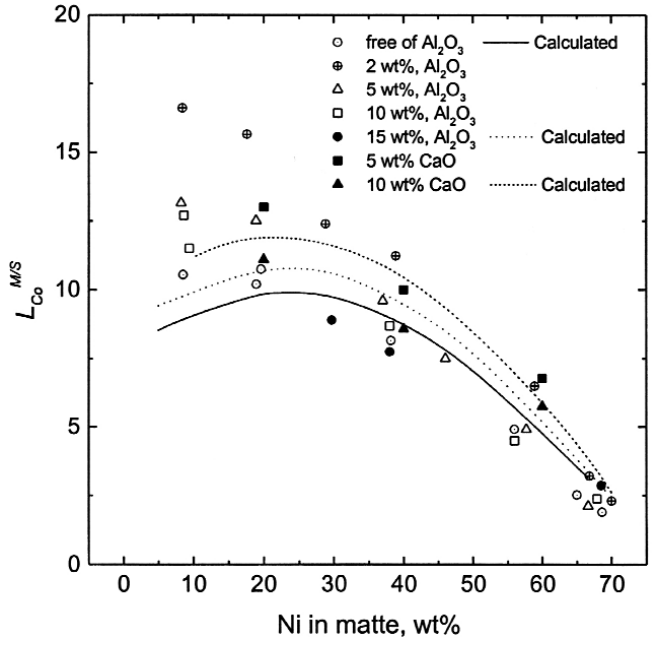

Figure 5. Comparison of experimental[21] and calculated cobalt distribution between nickel matte and silica-saturated iron silica slag

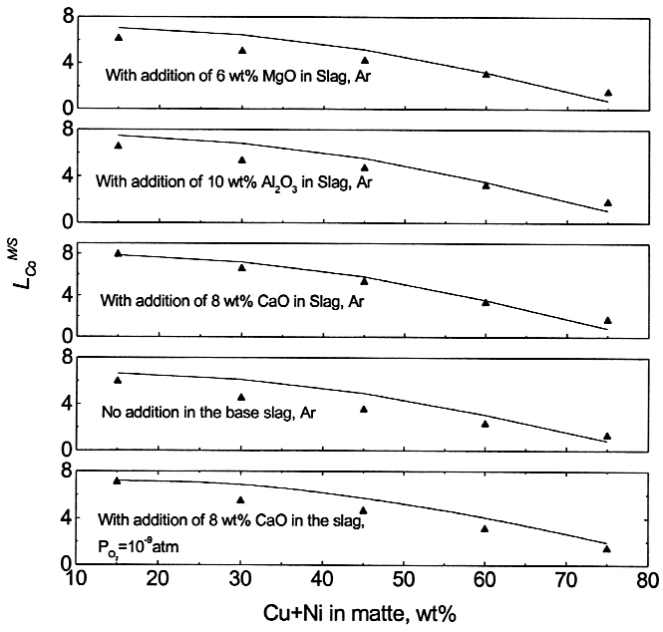

Figure 6. Comparison of experimental[22] and calculated cobalt distribution between copper-nickel matte and silica-saturated iron silica slag at 1250°C

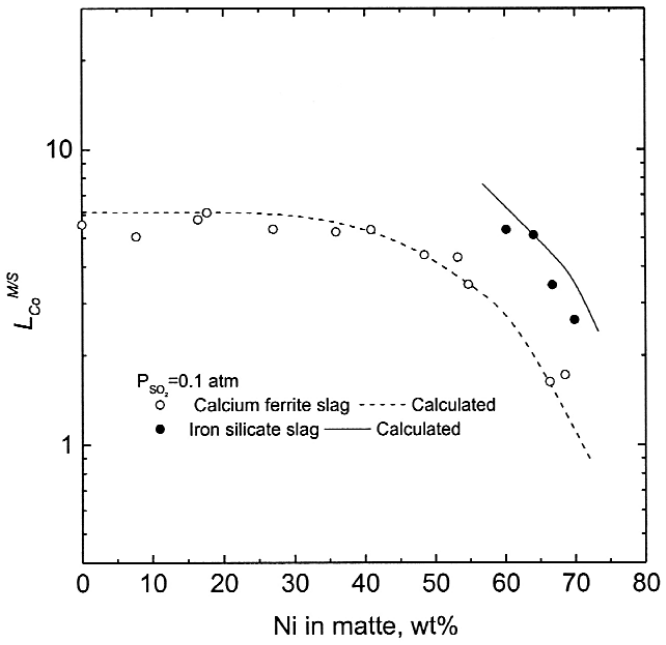

Figure 7. Comparison of experimental[23,24] and calculated distribution of cobalt between Ni matte/Fe_xO-SiO_2 slag and Ni matte/calcium ferrite slag

matte grade in the industrial processes. The curve in Figure 9 was calculated by using the MPE package based on the published operating parameters and the charge composition of mode 4 of the INCO flash smelting process[26]. Although direct comparison of the calculated curve with other industrial data is difficult due to the different operating conditions, such as difference in temperature, oxygen potentials, iron to silica ratio in the slags as well as nickel to copper ratio of the matte, there appears to be good agreement between calculated values and the industrial

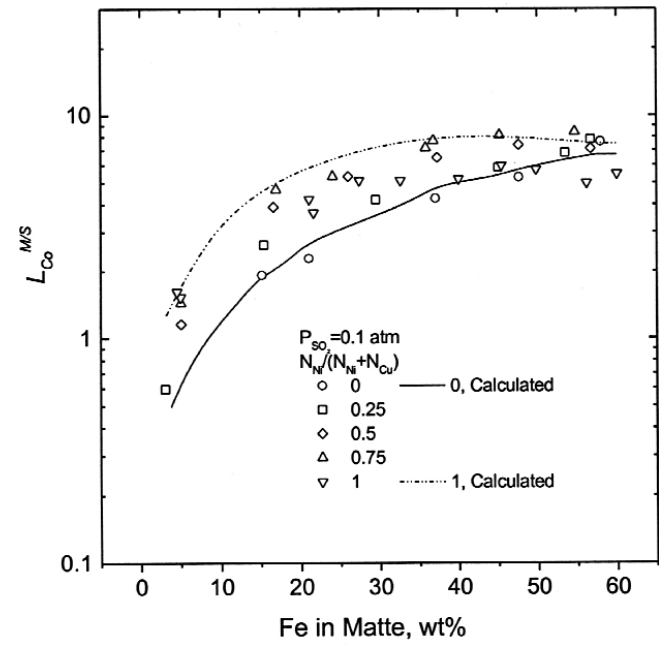

Figure 8. Comparison of experimental[25] and calculated distribution of cobalt between copper-nickel matte and FeO_x-SiO_2 slag as functions of Fe content in matte at 1300°C

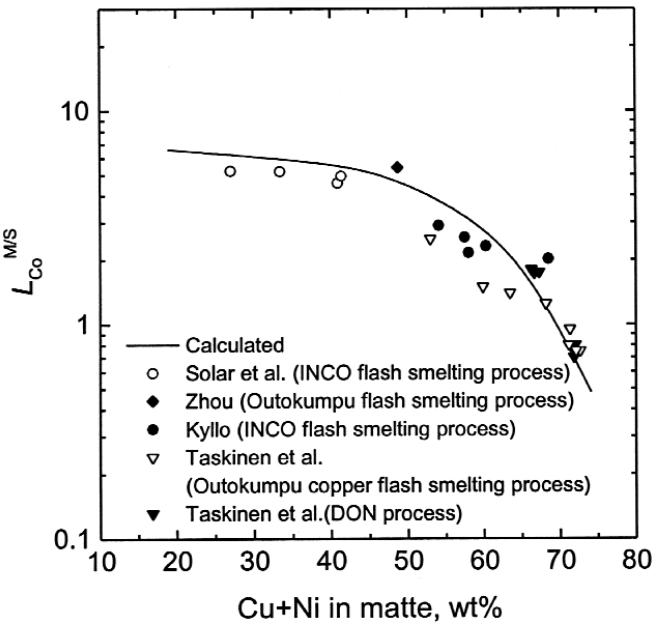

Figure 9. Distribution of cobalt in industrial smelting process[26-30]

data. This seems to suggest that the operating conditions of industrial smelting and converting processes were close to the equilibrium. In such cases, the equilibrium calculations could be used as a guide to the distribution behaviour of cobalt among phases under various conditions.

Calculated distribution coefficient of cobalt

Systematic experimental determination of cobalt distribution between matte and slag under different conditions is normally time consuming and costly. Moreover, finding an appropriate container material has always been one of the major problems in laboratory studies of matte-slag equilibria. The thermodynamic database developed in the present study makes it easy to evaluate the cobalt distribution between matte and slag at any given conditions of interest for plant practice.

Compared to the iron silicate slag, the calcium ferrite slag is a relatively new type of slag that is used in the Mitsubishi continuous copper-converting process. Although the calcium ferrite slag has not yet been used in the industrial nickel converting process, the possibility remains. Therefore, it is of interest to calculate the distribution of cobalt between copper-nickel matte and calcium ferrite slag under various conditions to examine the influence of the slag chemistry, oxygen partial pressure and temperature on the cobalt distribution.

Corresponding to the range of cobalt concentration in the industrial matte and slag, the cobalt concentration in matte and slag were set to be around 0.8 wt pct in our calculation. Figure 10 shows variations of distribution coefficients of cobalt as functions of iron to lime ratio in the slag when matte and slag are equilibrated at 1250°C and P_{O_2} = 10^{-8} atm. The temperature and oxygen partial pressure chosen lie between the temperatures and oxygen partial pressures normally encountered in copper and nickel smelting and converting processes. Figure 10 shows that the field of the matte-slag two-phase equilibrium is limited by dicalcium ferrite and spinel saturation at low and high Fe/CaO ratios, respectively. The cobalt distribution coefficients increase slightly with increasing of iron to lime ratio in the slag. The

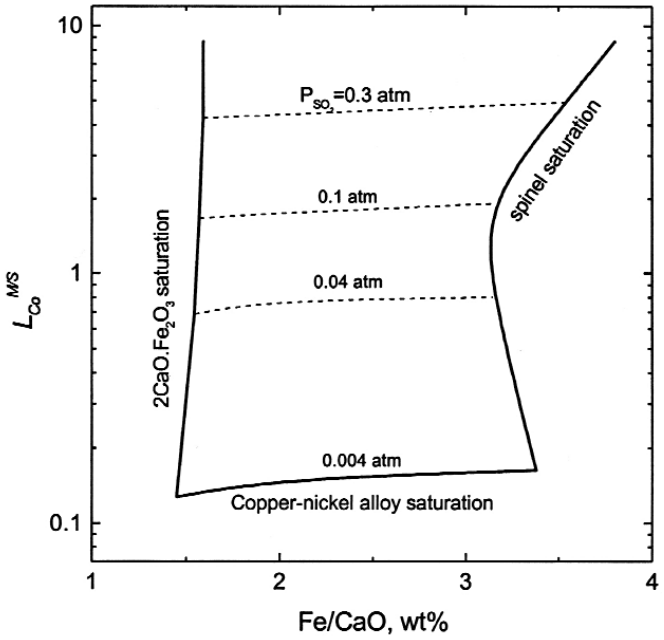

Figure 10. Calculated distribution of cobalt between matte and calcium ferrite slag at 1250°C, $P_{O_2}=10^{-8}$ atm and at infinite dilution of cobalt. Dashed lines show SO_2 isobars

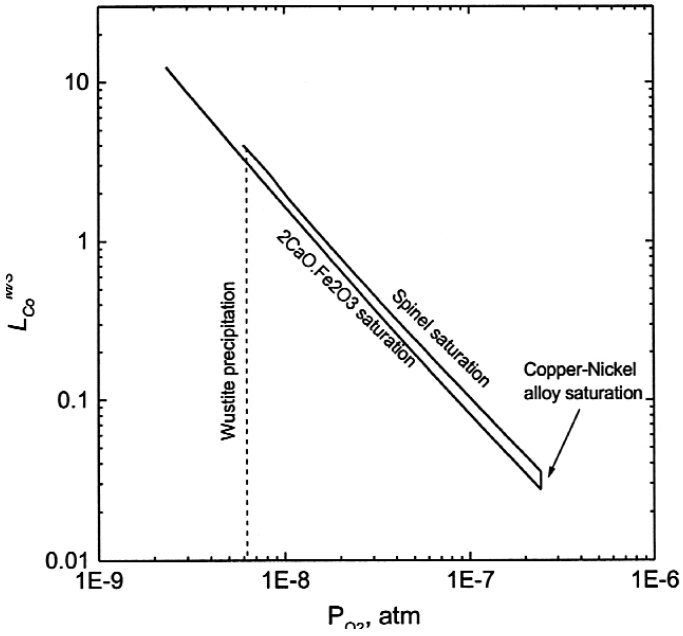

Figure 11. Calculated distribution of cobalt between matte and calcium ferrite slag at 1250°C, P_{SO_2}=0.1 atm and at infinite dilution of cobalt

SO_2 isobars over the two-phase field are also shown in the Figure. Another conclusion that can be drawn from Figure 10 is that the cobalt distribution decreases as SO_2 partial pressure decreases and reaches a considerably low value of about 0.1 in the region of copper-nickel alloy saturation. This suggests that the considerable loss of cobalt to the slag is inevitable in the smelting stage to produce the Bessemer matte.

Figure 11 shows the distributions of cobalt between matte and slag phases for the four-phase equilibria matte-slag-alloy-$2CaO.Fe_2O_3$ and matte-slag-alloy-spinel as a function of oxygen partial pressure. The distribution coefficient decreases as the oxygen partial pressure increases and this confirms the oxidic dissolution mechanism of cobalt solubility in the slag. At the same oxygen pressure, the distribution coefficients change slightly over the range from $2CaO.Fe_2O_3$ to spinel saturation.

The effect of temperature and the addition of SiO_2 and Al_2O_3 to calcium ferrite slag on the cobalt distribution coefficient have also been modelled. It was found that at the fixed oxygen partial pressure and matte grade, the distribution coefficient of cobalt decreased with increasing temperature, and this suggests that smelting and converting at low temperature will have advantages of increasing cobalt recovery from the slag.

The individual additions of SiO_2 or Al_2O_3 in the calcium ferrite slag increased the distribution coefficient of cobalt at all matte grades. This is likely be due to the strong interactions of SiO_2-CaO, SiO_2-FeO_x, Al_2O_3-CaO and Al_2O_3-FeO_x, which in turn decrease the interactions of CaO-CoO and FeO_x-CoO and cause the CoO activity to increase and, hence, decrease the solubility of cobalt in the slag. Modifying the slag chemistry through small additions of SiO_2 and Al_2O_3 could be a strategy to increase the cobalt recovery to the matte.

Conclusions

Thermodynamic models of the cobalt-containing slag and solid solution phases have been used to calculate CoO activity in multi-component slags. Comparison between the calculated CoO activity and the experimental data revealed that the models can provide good representation of the CoO activity in various slag systems, especially in the low CoO concentration region, which has the greater industrial relevance.

Incorporating the developed database into the MPE package enabled prediction of the cobalt distribution between matte and slag under various conditions. The MPE package represented the laboratory experimental data as well as the industrial observed distribution of cobalt between matte and slag phases. The good agreement between the calculation and the industrial data seems to suggest that the operating conditions of industrial smelting and converting processes are close to equilibrium.

The MPE package was also used to predict the distribution of cobalt between the copper-nickel matte and calcium ferrite slag at various conditions. Two types of diagrams produced are valid for both smelting and converting processes. Such information can be useful for development of new strategies for maximizing cobalt recovery from the discard slag and, furthermore, for development of new processes.

Acknowledgments

The authors thank Anglo Platinum, Impala Platium, Lonmin Platium, Kumba Resources, BHP Steel Ltd., Rio Tinto and CSIRO Minerals for providing the financial support for this work through the AMIRA.

References

1. ZHANG, L., JAHANSHAHI, S., LIM, M., BOURKE, B., WRIGHT, S. and SOMERVILLE, M., *Materials Forum*, vol. 25, 2001. pp. 136–153.
2. ZHANG, L., JAHANSHAHI, S., SUN, S., CHEN, C., BOURKE, B., WRIGHT, S. and SOMERVILLE, M., *Journal of Metals,* vol. 54, no. 11. 2002. pp. 51–56.
3. CHEN, C., ZHANG, L. and JAHANSHAHI, S., *Calphad XXXII*, La Malbaie, Quebec, Canada, 2003.
4. WANG, S. S., KURTIS, A. J. and TOGURI, J. M., *Can. Metall. Q*., vol. 12. no. 4. 1973. pp. 383–390.
5. WANG, S. S., SANTANDER, N. H. and TOGURI, J. *M., Metall. Trans*., vol. 5, 1974. pp. 261–265.
6. GRIMSEY, E. J. and TOGURI, J. M., *Can. Metall. Q*., vol. 27, no. 4. 1988. pp. 331–333.
7. GRIMSEY, E.J. and LIU, X., *Metall. Mater. Trans. B*, vol. 26B, 1995. pp. 229–234.
8. LIU, X. and GRIMSEY, E.J., *5th Int. Conf. On Molten Slags, Fluxes and Salts*, Sydney, 1997. pp. 709–713.
9. TEAGUE, K.C., SWINBOURNE, D.R. and JAHANSHAHI, S., *6th AusIMM*, Brisbane, 2000. pp. 67–73.
10. KATYAL, A. and JEFFES, J.H.E., *3rd Int. Conf. On Molten Slags and Fluxes*, Glasgow, Institute of Metals, London, 1989. pp. 46–55.
11. REDDY. R. G. and HEALY, G. W., *Can. Metall. Q*., vol. 20, 1981. pp. 135–143.
12. REDDY, R. G. and HEALY, G. W., *Metall. Trans. B*, vol. 12B, 1981. pp. 509–516.
13. PAGADOR, R. U., HINO, M. and ITAGAKI, K., *Proc. Nickel-Cobalt 97 Int. Symp.:Volume II, Pyrometallurgy Fundamentals and Process Development*, CIM, Sudbury, ON, Canada, 1997. pp. 63–75.
14. PAGADOR, R. U., Hino, M. and Itagaki, K., *Mater. Trans. JIM*, vol. 40, no. 3. 1999.pp. 225–232.
15. HENAO, H. M., HINO, M. and ITAGAKI, K., *Mater. Trans. JIM*, vol. 42, no. 9. 2001. pp. 1959–1966.
16. DERIN, B. and ONURALP, Y., *Scand. J. Metall*., vol. 31, 2002. pp. 12–19.
17. TAKEDA, A., ISHIWATA, Y. and YAZAWA, A., *Mater. Trans. JIM*, vol. 24, no. 7. 1983. pp. 518–528.
18. TEAGUE, K.C., SWINBOURNE, D.R. and JAHANSHAHI, S., *Metall. Mater. Trans. B*., vol 32B, 2001. pp. 47–54.
19. KONGOLI, F., DESSUREAULT, Y. and PELTON, A. D., *Metall. Mater. Trans. B*., vol. 29 B, 1998. pp. 591–601.
20. KONGOLI F. and PELTON A. D., *Metall. Mater. Trans. B*., vol. 30 B, 1999. pp. 443–450.
21. CELMER, R. S. and TOGURI, J. M., *IN nickel Metallurgy, Volume I—Extraction and Refining of Nickel*, TMS-CIM, 1986. pp. 147–163.
22. CHOI, N. and CHO, W. D., *Metall. Mater. Trans. B*, vol. 28B, 1997. pp. 429–438.
23. FONT, J. M., HINO, M. and ITAGAKI, K., *Mater. Trans. JIM*, vol. 39, no. 8. 1998. pp. 834–840.
24. FONT, J. M., HINO, M. and ITAGAKI, K., *Metall. Rev. MMIJ*, vol. 17, no. 2. 2001. pp. 106–115.
25. FONT, J. M., HINO, M. and ITAGAKI, K., *Metall. Mater. Trans. B*, vol. 31B, 2000. pp. 1231–1239.
26. SOLAR, M. Y., NEAL, R. J., ANTONIONI, T. N. and BELL, M. C., *Journal of Metals*, vol. 31, no. 1. 1979. pp. 26–32.
27. ZHOU, D., *Nonferrous Metals*, 1984. no. 4. pp. 4–8.
28. KYLLO, A. K., M.Sc. Thesis, University of British Columbia, Vancouver, BC, Canada. 1989.
29. TASKINEN, P., SEPPALA, K., LAULUMAA, J. and POIJARVI, J., *Trans. Instn. Min. Metall*., vol. 110, 2001. pp. C94–C100.
30. TASKINEN, P., SEPPALA, K., LAULUMAA, J. and POIJARVI, J., *Trans. Instn. Min. Metall*., vol. 110, 2001. pp. C101–C108.